Field-free charge polarization of mesoscopic rings

A. Matos-Abiague and J. Berakdar
Max-Planck Institut für Mikrostrukturphysik, Weinberg 2, 06120 Halle, Germany
(Received 2 June 2004; revised manuscript received 22 September 2004; published 23 November 2004)

We investigate the electron dynamics in a one-dimensional mesoscopic ring under the influence of short, linearly polarized half-cycle electromagnetic pulses. It is shown that the pulses induce a nonequilibrium coherent population of electronic states such that a time-dependent charge polarization of the ring is induced. The time-dependent charge oscillations persist after the pulses have diminished and decay on a time scale determined by the relaxation time. The overall duration of the charge polarization can be controlled by applying an appropriate train of half-cycle pulses. Furthermore, we show that the emission spectrum associated with the pulse-induced charge oscillations can be modulated appropriately by tuning the parameters of the driving pulses. It is shown theoretically how the induced charge polarization can in principle be utilized to measure experimentally the relaxation time of the system in a field-free manner.

DOI: 10.1103/PhysRevB.70.195338 PACS number(s): 78.67.−n, 42.65.Ky, 42.65.Re

I. INTRODUCTION

At low temperatures the phase coherence length L_ϕ of the charge carriers in a mesoscopic system increases significantly. This results in a series of quantum phenomena that are currently under intensive theoretical and experimental investigations. For instance, if in a mesoscopic ring (MR) L_ϕ is comparable to the ring size, the physical properties of the MR become dominated by quantum interferences of the electronic states. If the ring is threaded by a static magnetic field, the MR thermodynamic properties possess a periodic dependence on the magnetic flux. Prominent phenomena that emerge in this case are the so-called persistent currents[1–7] and the Aharonov-Bohm conductance oscillations which are the result of the free energy dependence on the magnetic flux.[8] The various facets of the persistent currents generated in MR's by a static magnetic field are well established. In particular, the electron-electron interaction,[9–11] the impurity scattering,[9] and disorder[5,10] effects on the persistent currents have been investigated in considerable detail. Persistent currents in carbon nanotube-based rings have recently been studied.[12] On the experimental side, several measurements have been reported of persistent currents.[13–16]

The dynamical effects produced by a *time-dependent* electric field acting on a MR threaded by a static magnetic field have been investigated in Refs. 17–20. In this case the existence of a direct nonequilibrium (charge) current has been theoretically predicted. The direct nonequilibrium current caused by nonlinear effects is an odd function of the static magnetic flux (as for the case of persistent currents). Consequently, this current vanishes if the static magnetic flux is zero.[18–20] Further investigations concerning the dynamical properties of MR's subject to external continuous-wave (CW) laser fields have also been reported.[21–23]

In the present paper we investigate the dynamics of charge carriers confined in a one-dimensional (1D) ballistic MR subject to linearly polarized half-cycle electromagnetic pulses (HCP's). An HCP is a strongly asymmetric monocycle pulse consisting of a very short, strong half-cycle (we refer to this part as an HCP), followed by a second half-cycle of an opposite polarity (the tail of the HCP). This second part of the pulse can be attenuated and stretched substantially (in time) by means of optical gating techniques.[24] Since the HCP tail is very weak and very long (compared to the relaxation time of MR's), it hardly influences the electron dynamics. Consequently, once the HCP has passed by, the system behaves as under zero-field conditions. Presently HCP's are available with durations in the (sub)picosecond regime and with a peak field up to several hundreds of kV/cm.[25] As well, trains of HCP's are shown to be experimentally feasible.[26–28]

The findings reported in this paper can be summarized as follows: the application of a short linearly polarized HCP on a ballistic thin MR induces a charge polarization that persists much longer than the pulse duration. For this reason we also refer to the post-pulse charge polarization as the field-free polarization. We consider the case where the round-trip time (nanoseconds) of the unperturbed charge carriers is much longer than the pulse duration τ_d (picoseconds). In this situation it has been shown that the pulse shape is irrelevant for the charge dynamics and the HCP can be modeled by an *instantaneous kick* applied at the time t_1 and having the strength $\mathbf{p}=-\int_0^{\tau_d}\mathbf{F}(t)dt$.[26,27,29–31] Here $\mathbf{F}$ is the electric field amplitude of the pulse. This is the essence of the so-called impulsive approximation whose validity has already been demonstrated numerically.[29,30] In the impulsive regime, applying a short HCP delivers a momentum transfer (or *kick*) to the charge carriers in the ring which results in time-dependent charge oscillations. As shown below explicitly, the deviation from the equilibrium state is governed mainly by the strength of the pulse. The time scale for the decay of the induced charge oscillations is governed by the relaxation time of the system. No total charge current is induced in the ring when linearly polarized HCP's are applied with a fixed polarization axis. As one can expect from an intuitive point of view, the application of a linearly polarized pulse does not destroy the clockwise-counterclockwise symmetry of the charge carriers paths in the ring and thus the total current vanishes.

II. POSTPULSE POLARIZATION

We consider an isolated 1D ballistic mesoscopic ring at low temperature ($T\approx 0$ K). For a thin enough ring with a

width $d \ll \rho_0$, the angular motion is much slower than the radial motion and, consequently, both degrees of freedom can be adiabatically decoupled. Furthermore, if d is smaller than the Fermi wavelength, then the MR becomes a single-channel 1D ring. In what follows we limit our analysis to the case of a single-channel 1D ballistic ring. Despite the relative simplicity of this model, it has been shown to provide valuable physical insight into the description of thin MR's in the ballistic regime.[1–6,15,21] A further advantage of using the single-channel model is that analytical results can be obtained and analyzed. In the conclusion section we will comment on the effects expected when 2D rings are used. At $t = t_1$ a linearly polarized HCP with $\mathbf{F} \| x$ is applied to the ring. The duration of the pulse is assumed to be much shorter than the ballistic time τ_F, where τ_F is the time needed by a particle at the Fermi level for completing one turn around the ring. This requirement is realizable experimentally since for typical ballistic rings τ_F is of the order of several tens of picoseconds[15,32] and typical HCP's employed in this work and experimentally feasible are as short as 1 ps.[25] Consequently, one can safely treat the interaction of the charge carrier with the HCP within the impulsive approximation (IA). In addition, in our case the basic quantity for the the study of the charge dynamics is the time-dependent single-particle wave function Ψ. Mathematically speaking, the IA means that Ψ obeys a time-dependent Schrödinger equation describing rotational states that are kicked instantaneously at time t_1 with a kick strength p[26,27,29]—i.e.,

$$i\hbar \frac{\partial \Psi}{\partial t} = \left[-\frac{\hbar^2}{2m^* \rho_0^2} \frac{\partial^2}{\partial \theta^2} - q\rho_0 \varepsilon(t) \cos\theta \right] \Psi, \tag{1}$$

where

$$\varepsilon(t) = p\,\delta(t - t_1). \tag{2}$$

In Eqs. (1) and (2), ρ_0 is the radius of the ring, $\delta(x)$ denotes the Dirac function, and θ is the polar angle of the charge carrier measured with respect to the HCP polarization axis. The effective mass and charge of the carriers are denoted by m^* and q, respectively. Henceforth we assume without loss of generality that $t_1 = 0$.

We note that Eq. (1) corresponds, actually, to a kicked rigid rotor (KRR). Dipolar molecules interacting with HCP's are also approximated by a KRR. It has been numerically shown in Ref. 30 that for molecules with a rotational period much larger than the duration of the pulses, the IA is excellent. The situation discussed here is quite analogous and one can expect the IA to be indeed valid.

The solutions of Eq. (1) obey the matching condition

$$\Psi(\theta, t = 0^+) = \Psi(\theta, t = 0^-) e^{i\alpha \cos\theta}, \tag{3}$$

where $\alpha = q\rho_0 p/\hbar$ and $t = 0^-$ and $t = 0^+$ refer, respectively, to the times just before and right after the application of the pulse.

The solution $\Psi_{m_0}(\theta, t)$ of Eq. (1) that corresponds to a particle initially residing in the (m_0)th orbital state can be expanded in terms of the ring stationary eigenstates (in the absence of the HCP) as

$$\Psi_{m_0}(\theta, t) = \frac{1}{\sqrt{2\pi}} \sum_{m=-\infty}^{\infty} C_m(m_0, t) e^{im\theta} e^{-iE_m t/\hbar}. \tag{4}$$

Here we denoted the orbital energies of the unperturbed states by E_m, where

$$E_m = \frac{\hbar^2 m^2}{2m^* \rho_0^2}, \quad m = 0, \pm 1, \pm 2, \ldots . \tag{5}$$

Taking into account the matching condition stated in Eq. (3) and after applying the expansion theorem one finds that the expansion coefficients are given by

$$C_m(m_0, t) = \begin{cases} \delta_{m,m_0} & \text{for } t \leq 0, \\ i^{m_0 - m} J_{m - m_0}(\alpha) & \text{for } t > 0, \end{cases} \tag{6}$$

with $J_l(x)$ representing the Bessel functions and $\delta_{m,n}$ the Kronecker symbol. In obtaining Eq. (6) the identity in Eq. (A2) has been utilized.

Upon applying the HCP the energy spectrum of the particles is rearranged. Specifically, the energy corresponding to a particle initially in the (m_0)th state evolves as

$$\begin{aligned} E_{m_0}(t) &= \langle \Psi_{m_0}(\theta, t) | H | \Psi_{m_0}(\theta, t) \rangle \\ &= i\hbar \left\langle \Psi_{m_0}(\theta, t) \left| \frac{\partial}{\partial t} \right| \Psi_{m_0}(\theta, t) \right\rangle. \end{aligned} \tag{7}$$

The substitution of Eqs. (4)–(6) in Eq. (7) leads to the post-pulse energy (i.e., for $t > 0$)

$$E_{m_0}(t > 0) = \frac{\hbar^2}{2m^* \rho_0^2} \sum_{m=-\infty}^{\infty} [m J_{m_0 - m}(\alpha)]^2. \tag{8}$$

The infinite sum involved in Eq. (8) can be performed exactly [see Eq. (A3) in the Appendix] and the energy corresponding to a particle initially in the (m_0)th state is given by

$$E_{m_0}(t) = \begin{cases} \dfrac{\hbar^2 m_0^2}{2m^* \rho_0^2} & \text{for } t \leq 0, \\ \dfrac{\hbar^2}{2m^* \rho_0^2} \left(m_0^2 + \dfrac{\alpha^2}{2} \right) & \text{for } t > 0. \end{cases} \tag{9}$$

Recalling that $\alpha = q\rho_0 p/\hbar$ we can write, for the particle energy upon the pulse,

$$E_{m_0}(t > 0) = E_{m_0}(t < 0) + \frac{q^2}{2} \frac{p^2}{2m^*}. \tag{10}$$

Thus, applying an HCP to the ring shifts the unperturbed energy spectrum by an amount that scales quadratically with the strength of the pulse and does not depend on the size of the ring. The initial degeneracy is preserved after the pulse is applied. Furthermore, since $E_{m_0}(t > 0)$ grows quadratically with m_0, Eq. (10) dictates that the energy of a particle at the Fermi level (for which $m_0 \approx N/4$) be affected only marginally by the pulse if $(N/4)^2 \gg \alpha^2/2$. For small p and for rings containing a large number of particles this condition may well be met—e.g., as for the explicit numerical illustrations discussed below. To inspect the structure of the coherent states created by the pulse we inspect Eqs. (4) and (6). Under

the condition $m'=|m-m_0|\gg\alpha$ we have from Eqs. (6) and (A1) that

$$|C_m(m_0,t>0)|\approx\frac{1}{\sqrt{2\pi m'|}}\left(\frac{e\alpha}{2m'}\right)^{m'},\quad m'\gg\alpha. \tag{11}$$

In the weak-field regime p is small and, consequently, α is small too. In such a situation the condition $m'=|m-m_0|\gg\alpha$ is easily reached and $|C_m(m_0,t>0)|^2$ rapidly decays when increasing the value $|m-m_0|$; i.e., only few states (labeled by m) around m_0 contribute to the coherent population created by the pulse. It is not difficult to prove from Eqs. (4)–(6) that $\Psi_{m_0}(\theta,t)=\Psi_{-m_0}(-\theta,t)$; i.e., the clockwise-counterclockwise symmetry of the charge carrier is preserved after the application of the pulse, and therefore, currents carried by particles initially in the m_0 and $-m_0$ states compensate each other. This fact together with the degeneracy of the states [see Eq. (9)] confirms the intuitive expectation that no total current will be induced in the ring.

In order to characterize the degree of polarization in the direction of the pulse (i.e., along the x axis), we introduce the localization parameter

$$\langle\cos\theta\rangle_{m_0}(t)=\int_0^{2\pi}|\Psi_{m_0}(\theta,t)|^2\cos\theta d\theta. \tag{12}$$

This parameter is the analog to the parameter commonly used for characterizing molecular orientation.[30,33] Thus, $\langle\cos\theta\rangle_{m_0}(t)$ is a measure of how strong a particle occupying initially the (m_0)th state localizes along the x direction upon the application of the pulse. The dynamical quantity $\langle\cos\theta\rangle_{m_0}(t)$ varies in the interval $[-1,1]$. The extremal values -1 and 1 are acquired when the particle is perfectly localized at the angles $\theta=\pi$ and $\theta=0$, respectively. Note, however, that $\langle\cos\theta\rangle_{m_0}(t)=0$ does not necessary mean that the particle is localized at $\theta=\pm\pi/2$. In such a case the only conclusion is that, statistically, the particle is distributed symmetrically with respect to the y axis, meaning that the polarization in the x direction vanishes. Note also that the dipole moment μ_{m_0} along the x axis corresponding to a particle initially in the (m_0)th stationary state is proportional to $\langle\cos\theta\rangle_{m_0}(t)$. More precisely, μ_{m_0} is given by

$$\mu_{m_0}(t)=q\rho_0\langle\cos\theta\rangle_{m_0}(t). \tag{13}$$

After some mathematical manipulations one can obtain from Eqs. (4)–(6) and (12) the relation

$$\langle\cos\theta\rangle_{m_0}(t)=\Theta(t)\alpha h(\Omega)\sin\left[\frac{2\pi t}{\tau_p}\right]\cos\left[\frac{4\pi m_0 t}{\tau_p}\right], \tag{14}$$

where $\Theta(x)$ denotes the Heaviside step function,

$$\Omega=\alpha\sqrt{2-2\cos[4\pi t/\tau_p]},\quad \tau_p=\frac{4\pi m^*\rho_0^2}{\hbar}, \tag{15}$$

and

$$h(\Omega)=J_0(\Omega)+J_2(\Omega). \tag{16}$$

In obtaining Eq. (14) we exploited the relation stated by Eq. (A4).

From Eq. (14) we deduce that $\langle\cos\theta\rangle_{m_0}(t)=\langle\cos\theta\rangle_{-m_0}(t)$. Therefore, the contributions of particles initially in the m_0 and $-m_0$ states to the polarization interfere constructively and a nonvanishing total polarization is generated. The total HCP-induced dipole moment along the x axis is given by

$$\mu(t)=\sum_{m_0,\sigma}f(m_0,t)\mu_{m_0}(t), \tag{17}$$

where σ refers to the spin of the particle, f represents the nonequilibrium distribution function, and $\mu_{m_0}(t)$ is given by Eq. (13). If the MR is thin enough, the lowest subband accommodates all the electrons. In this case it has been shown that the electron-electron interaction plays a subsidiary role at low temperatures T.[6,11]

When a MR is irradiated by the HCP, the charge carriers are promoted to excited states and start to relax after the HCP has passed by. For $T\approx 0$ K and for relatively weak pulses $[\hbar^2\alpha^2/(4m^*\rho_0^2)\ll E_F]$, the relaxation time approximation is a reasonable way for the evaluation of the nonequilibrium distribution function.[32,34,35] In principle the relaxation of the system may occur via various mechanisms—e.g., electron-phonon scattering, electron-electron scattering, etc. Here these relaxation processes are incorporated in a single (averaged) parameter, the relaxation time τ_{rel} that is included at a phenomenological level. In fact, as shown below, the decay of the induced polarization can be monitored experimentally, providing thus an experimental possibility for measuring τ_{rel} (cf. discussion in Sec. IV).

Within the relaxation time approximation, the nonequilibrium distribution function is determined by the Boltzmann equation

$$\frac{\partial f(m_0,t)}{\partial t}=\frac{f(m_0,t)-n_F(m_0)}{\tau_{rel}}, \tag{18}$$

where τ_{rel} represents the relaxation time and

$$n_F(m_0)=\left[1+\exp\left(\frac{E_{m_0}(t\leqslant 0)-\eta_0}{k_BT}\right)\right]^{-1} \tag{19}$$

denotes the Fermi-Dirac distribution function corresponding to the equilibrium. In the equation above, T, k_B, and η_0 represent the temperature, the Boltzmann constant, and the chemical potential (for $t\leqslant 0$), respectively.

Equation (18) has to be complemented with the boundary condition specifying the value of the distribution function right after application of the pulse:

$$f(m_0,0^+)=n_F^{(1)}(m_0)=\left[1+\exp\left(\frac{E_{m_0}(t>0)-\eta_1}{k_BT}\right)\right]^{-1}. \tag{20}$$

The values of the chemical potentials η_0 and η_1 depend on the physical nature of the system. If the ring is connected to a reservoir of particles, for example, the chemical potential is fixed and $\eta_0=\eta_1$. In the particular case of our interest, in which the MR is isolated, the chemical potentials η_0 and η_1 have to be calculated, however, by requiring the number of particles N in the ring to be a constant. Thus, for a given isolated ring with N particles, η_0 is a function of the tem-

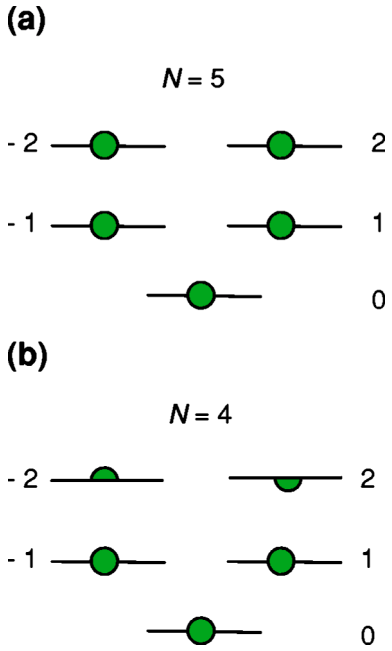

FIG. 1. (Color online) Filling of the energy levels (denoted by labeled lines) at $T=0$ K for the case of N spinless particles (symbolized by dots). (a) N is an odd number and all the occupied levels are completely filled. (b) N is an even number and, because of the energy degeneracy, the highest occupied levels are half-filled.

perature, while η_1 depends on both the temperature and pulse amplitude.

It is worth noting that in the case of an isolated MR the relaxation mechanism has to include, necessarily, inelastic scattering. The interaction of the carriers with the phonons is then crucial for the estimation of τ_{rel}. Here, however, we consider, as mentioned above, τ_{rel} as a phenomenological parameter.

Taking into account that the value of the dipole moment before the application of the pulse (i.e., its equilibrium value) is zero and after solving Eq. (18) with the boundary condition expressed in Eq. (20), one can rewrite Eq. (17) as follows:

$$\mu(t) = e^{-t/\tau_{rel}} \sum_{m_0,\sigma} n_F^{(1)}(m_0)\mu_{m_0}(t). \tag{21}$$

At zero temperature only the lowest-lying states are occupied. In such a case the sum in Eq. (21) can be performed analytically by taking into account the dependence of the filling of the levels below the Fermi level on whether the carriers are spinless or spin-$\frac{1}{2}$ particles as well as on the number N of particles in the ring.

In the case of spinless particles at $T=0$ K the filling of the levels below the Fermi level depends on whether there is an odd or even number of particles in the ring (we recall that we are considering an isolated ring and therefore the number of particles is constant). In the case N is an odd number all the occupied levels are completely filled [see Fig. 1(a)] and Eq. (21) reduces to

$$\mu(t) = e^{-t/\tau_{rel}} \sum_{m_0=-(N-1)/2}^{(N-1)/2} \mu_{m_0}(t). \tag{22}$$

Upon substituting Eqs. (13) and (14) into Eq. (22) one obtains an expression for the dipole moment $\mu_o(N,t)$ in the case the number of the spinless particles in the ring is odd—namely,

$$\mu_o(N,t) = -\Theta(t) q\alpha\rho_0 h(\Omega) \sin\left[\frac{2\pi N t}{\tau_p}\right] e^{-t/\tau_{rel}}. \tag{23}$$

In the case of an even number of spinless particles the highest occupied levels are half-filled [see Fig. 1(b)] **(**due to the energy degeneracy [see Eq. (9)]**)**. Consequently, in such a case Eq. (21) reduces to

$$\mu(t) = e^{-t/\tau_{rel}} \sum_{m_0=-(N-2)/2}^{(N-2)/2} \mu_{m_0}(t) + \frac{1}{2}[\mu_{-N/2}(t) + \mu_{N/2}(t)]. \tag{24}$$

From Eqs. (13), (14), and (24) we deduce the relation for the dipole moment $\mu_e(N,t)$ in the case of an even number of spinless particles in the ring:

$$\mu_e(N,t) = -\Theta(t) q\alpha\rho_0 h(\Omega) \sin\left[\frac{2\pi N t}{\tau_p}\right] \cos\left[\frac{2\pi t}{\tau_p}\right] e^{-t/\tau_{rel}}. \tag{25}$$

For the case of spin-$\frac{1}{2}$ particles the induced dipole moment can be written as

$$\mu^{\sigma}(t) = \mu^{\uparrow}(t) + \mu^{\downarrow}(t), \tag{26}$$

where $\mu^{\uparrow}(t)$ and $\mu^{\downarrow}(t)$ refer to the contributions from the spin-up and spin-down configurations, respectively. Four cases regarding the number of particles in the ring need to be considered separately. The situation is shown in Fig. 2, where the filling of the levels by spin-up [yellow (light) circles and semicircles and spin-down [blue (dark) circles and semicircles] particles is sketched. The comparison between Figs. 1 and 2 reveals the possibility of expressing the dipole moment corresponding to the case of spin-$\frac{1}{2}$ particles as a function of the dipole moment corresponding to the spinless particles case (see also Ref. 7). We now study in details the four cases of interest.

(1) *An even number of pairs*—i.e., $N=0(\mathrm{mod}\ 4)$. In such a case one easily obtains from the comparison of Figs. 1 and 2(a) that the contributions to the dipole moment resulting from up spins and down spins are

$$\mu^{\uparrow}(N,t) = \mu^{\downarrow}(N,t) = \mu_e(N/2,t); \tag{27}$$

i.e., they are identical and each is equal to the dipole moment corresponding to the case of $N/2$ spinless particles (note that $N/2$ is even).

(2) *An even number of pairs plus an extra particle*—i.e., $N=1(\mathrm{mod}\ 4)$. From Figs. 1 and 2(b) it follows that

$$\mu^{\uparrow}(N,t) = \mu_o((N+1)/2,t),$$

$$\mu^{\downarrow}(N,t) = \mu_e((N-1)/2,t). \tag{28}$$

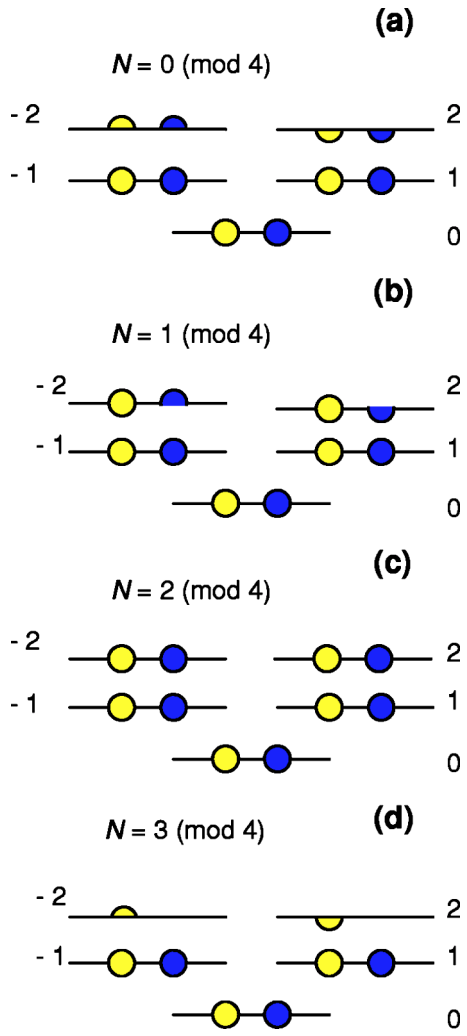

FIG. 2. (Color online) Filling of the energy levels (labeled solid lines) at $T=0$ K for the case of N spin-$\frac{1}{2}$ particles. Yellow (light) and blue (dark) circles and semicircles correspond to spin-up and spin-down particles, respectively. (a), (b), (c), and (d) correspond to the cases $N=0(\text{mod } 4)$, $N=1(\text{mod } 4)$, $N=2(\text{mod } 4)$, and $N=3(\text{mod } 4)$ particles.

(3) *An odd number of pairs*—i.e., $N=2(\text{mod } 4)$. Comparing Figs. 1 and 2(c) we conclude that

$$\mu^{\uparrow}(N,t) = \mu^{\downarrow}(N,t) = \mu_o(N/2,t); \tag{29}$$

i.e., the induced dipole moments associated with spin-up and spin-down particles are identical and each is equal to the dipole moment corresponding to the case of $N/2$ spinless particles (note that $N/2$ is odd).

(4) *An odd number of pairs plus an extra particle*—i.e., $N=3(\text{mod } 4)$. From the comparison of Figs. 1 and 2(d) one obtains that

$$\mu^{\uparrow}(N,t) = \mu_e((N+1)/2,t),$$

$$\mu^{\downarrow}(N,t) = \mu_o((N-1)/2,t). \tag{30}$$

Taking into account the four cases discussed above, one obtains from Eq. (26) that for the case of spin-$\frac{1}{2}$ particles, the total induced dipole moment $\mu^{\sigma}(t)$ can be expressed in terms of dipole moments for the spinless case [Eqs. (23) and (25)]. The exact relationships are as follows:

$$\mu^{\sigma} = \begin{cases} 2\mu_e\left(\frac{N}{2},t\right) & \text{if } N=0(\text{mod } 4), \\ \mu_o\left(\frac{N+1}{2},t\right) + \mu_e\left(\frac{N-1}{2},t\right) & \text{if } N=1(\text{mod } 4), \\ 2\mu_o\left(\frac{N}{2},t\right) & \text{if } N=2(\text{mod } 4), \\ \mu_e\left(\frac{N+1}{2},t\right) + \mu_o\left(\frac{N-1}{2},t\right) & \text{if } N=3(\text{mod } 4). \end{cases} \tag{31}$$

For a typical MR, τ_p is in the nanosecond regime whereas the HCP duration and the buildup as well as the decay time of the polarization are in the picosecond time scale (as demonstrated below). Therefore, the time domain of relevance here corresponds to $t \ll \tau_p$. In such a time domain ($t \ll \tau_p$) the dependence of the induced polarization on the parity of the number of particles N becomes irrelevant [compare Eqs. (23) and (25)]. More precisely, for $t \ll \tau_p$ and for $N \gg 1$ [i.e., if $(N\pm 1)/N \approx 1$] one deduces from Eqs. (23)–(31) that all four cases in Eq. (31) tend to the same approximate expression

$$\mu^{\sigma}(N,t) \approx -2\alpha q \rho_0 \Theta(t)[J_0(\Omega) + J_2(\Omega)]\sin\left[\frac{\pi N t}{\tau_p}\right] e^{-t/\tau_{rel}}. \tag{32}$$

III. EMISSION PROPERTIES

The dynamical polarization in a MR induced by a *single* HCP decays within a time of the order of the relaxation time τ_{rel}. These charge oscillations can, however, be sustained for longer time periods if a sequence of HCP's is applied. The oscillating charge density generates electromagnetic radiation. The characteristics of these radiation can be, to a certain extent, controlled by appropriately designing the sequence of HCP's. In this sense the driven MR can serve as a controllable source of electromagnetic radiation. Furthermore, the creation of a planar array of isolated MR's (similar arrays but including connected rings have already been experimentally realized[16]) could resonantly increase the emission intensity. It is worth noting also that the optical emission from quantum rings has already been experimentally studied in different situations.[36,37] To explore the emission properties in more detail we consider a driving field consisting of a quasiperiodic train of HCP's linearly polarized in the x direction and applied at $t=0$. Quasiperiodicity means that the HCPs sequence lasts for a certain time lap ΔT. Within the time ΔT the HCP train is periodic with a period T_p. Of a particular interest is the case where T_p is much longer than the relaxation time τ_{rel}. Designing the pulse train such that $T_p \gg \tau_{rel}$, the task of describing the time evolution of the system under

the action of the HCP's train reduces to the treatment of the system evolution triggered by one pulse and then exploiting the time periodicity within ΔT.

For spin-$\frac{1}{2}$ particles, the charge polarization $\mu_k(t)$ of the MR induced by a periodic train of k HCP's with period $T_p \gg \tau_{rel}$ is obtained from the one-HCP polarization Eq. (32) through the relation

$$\mu_k(t) = \sum_{j=0}^{k-1} \mu^\sigma(t - kT_p), \tag{33}$$

where the dependence on N has been omitted for brevity.

The emission spectrum $I(\omega)$ produced by the charge oscillations in the MR is given by

$$I(\omega) \sim |\mu_k(\omega)|^2, \tag{34}$$

where $\mu_k(\omega)$ is the Fourier transform of $\mu_k(t)$.

Taking into account the properties of the Fourier transform one verifies that

$$\mu_k(\omega) = \mu^\sigma(\omega) \frac{\sin\left(\frac{k\omega T_p}{2}\right)}{\sin\left(\frac{\omega T_p}{2}\right)} e^{-i[(k-1)/2]\omega T_p}, \tag{35}$$

where

$$\mu^\sigma(\omega) = \int_{-\infty}^{\infty} \mu^\sigma(t) e^{-i\omega t} dt \tag{36}$$

is the Fourier transform of the polarization $\mu^\sigma(t)$ induced by a single HCP as given by Eq. (32). Then Eq. (34) can be written as follows:

$$I(\omega) \sim Y(\omega) \left[\frac{\sin\left(\frac{k\omega T_p}{2}\right)}{\sin\left(\frac{\omega T_p}{2}\right)} \right]^2. \tag{37}$$

Here we introduced the function $Y(\omega) = |\mu^\sigma(\omega)|^2$. From Eq. (37) it is evident that the emission spectrum has peaks at the integer harmonics ($\omega = n\omega_0, \omega_0 = 2\pi/T_p$, $n = 0, 1, 2, \ldots$). The amplitudes of these peaks are determined by the modulation function $k^2 Y(\omega)$.

In general, the Fourier transform in Eq. (36) must be evaluated numerically. However, for the case of very weak pulses ($\alpha \ll 1/2$) we conclude that $\Omega \ll 1$ and the Bessel functions in Eq. (32) can be approximated by[38]

$$J_\nu(\Omega) \approx \frac{1}{\Gamma(\nu+1)} \left(\frac{\Omega}{2}\right)^\nu, \quad \nu \neq -1, -2, -3, \ldots. \tag{38}$$

In this limit ($\Omega \ll 1$) $Y(\omega)$ acquires the analytical expression

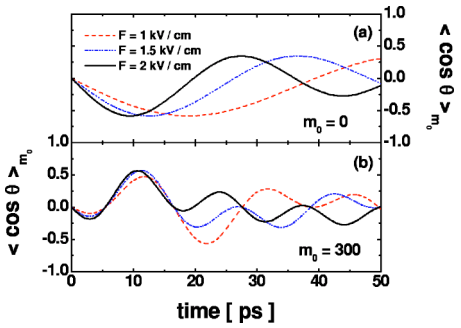

FIG. 3. (Color online) Time dependence of the localization parameter $\langle \cos\theta \rangle_{m_0}$.

$$Y(\omega) = \frac{(2\pi\alpha q \rho_0 N)^2}{\left(\frac{\tau_p}{\tau_{rel}^2} + \frac{\pi^2 N^2}{\tau_p} - \omega^2 \tau_p\right)^2 + 4\omega^2 \frac{\tau_p^2}{\tau_{rel}^2}}. \tag{39}$$

Therefore, we conclude that for ($\alpha \ll 1/2$) the modulation function Y has a maximal value Y_{max} at the frequency ω_{max}, where

$$k^2 Y_{max} = (k\alpha q \ \rho_0 \tau_{rel})^2 \tag{40}$$

and

$$\frac{\omega_{max}}{\omega_0} = \sqrt{\left(\frac{NT_p}{2\tau_p}\right)^2 - \left(\frac{T_p}{2\pi\tau_{rel}}\right)^2}. \tag{41}$$

Note, however, that as ω_{max} must be a real number, the maximum, Eq. (40), exists only if $\tau_{rel} \geqslant \tau_p/(\pi N)$. It is also worthwhile to note that although the amplitude of the modulation function depends on the pulse amplitude, its form is determined exclusively by the ring parameters.

IV. NUMERICAL RESULTS

For a concrete demonstration of the above findings we calculated the HCP-induced polarization for a ballistic GaAs-AlGaAs ring similar to that used in the experiment reported in Ref. 15. We stress, however, that the ring used in Ref. 15 is not a single-channel ring, since its width $d \approx 0.16$ μm is greater than the corresponding Fermi wavelength $\lambda_F \approx 0.042$ μm. Here we consider a ring with the same parameters as in Ref. 15 but assume its width $d \ll \lambda_F$, so that only the lowest channel participates in the dynamics of the system. The ring radius is $\rho_0 = 1.35$ μm, whereas the electron effective mass is $m^* = 0.067 m_e$, and $N = 1400$. Sine-square-shaped HCP's with a time duration of 1 ps are employed. Zero temperature is considered in all calculations.

The time dependence of the localization parameter $\langle \cos\theta \rangle_{m_0}$ corresponding to the ground state ($m_0 = 0$) is displayed in Fig. 3(a) for different values of the field amplitude F of the HCP. As evidenced by this figure, a particle initially in the ground stationary state reaches its maximum localization around $\theta = \pi$ after a time of the order of 20 ps for a peak field $F = 1$ kV/cm. When stronger fields are applied, the localization of the particle oscillates faster with time. If $F = 2$ kV/cm, the particle localizes roughly along the $-x$ and

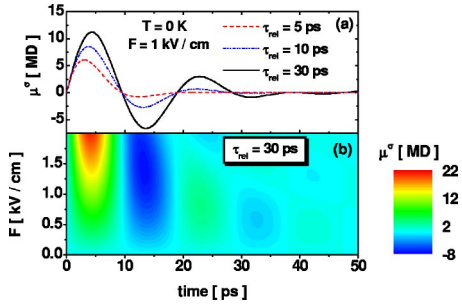

FIG. 4. (Color online) Time dependence of the dipole moment μ^{σ} corresponding to the case of spin-$\frac{1}{2}$ particles for different values of the relaxation time τ_{rel} (a) and with varying the pulse strength F (b).

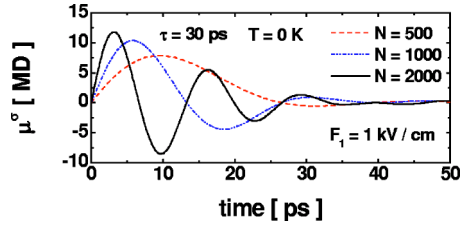

FIG. 5. (Color online) Time dependence of the dipole moment μ^{σ} corresponding to the case of spin-$\frac{1}{2}$ particles for different values of the number of particles, N, in the ring.

along the x direction after times of about 8 and 27 ps, respectively.

We note that with an increasing HCP field strength the electronic states undergo a larger momentum and energy change [cf. Eq. (9)]. Therefore the oscillations in the charge-density localization parameter $\langle \cos\theta \rangle_{m_0}$ become faster with increasing F. The same argument applies if initially (before applying the HCP's) the carriers reside in a high-angular-momentum state. In this case the localization $\langle \cos\theta \rangle_{m_0}$ has a fast oscillatory behavior in time, even for small fields. This situation is illustrated in Fig. 3(b), in which case $m_0=300$. In this context it is important to mention that the localization parameter $\langle \cos\theta \rangle_{m_0}$ is strictly periodic with a period determined by τ_p [see Eq. (14)]. However, since $\tau_p \approx 13.26$ ns is much longer than the typical relaxation time τ_{rel}, the field-free (postpulse) charge oscillations decay before the τ_p periodic dependence becomes apparent. Figure 3(b) indicates that stronger fields lead faster to a localization of the charge carriers. We remark, however, that a strong field strength if not necessarily a prerequisite for stronger localization.

Having discussed the general properties of the localization parameter we focus now on the details of the induced electric dipole. Using the relaxation time approximation we evaluated the time dependence of the total dipole moment μ^{σ} for different values of τ_{rel} and for varying pulse field amplitudes in Figs. 4(a) and 4(b), respectively. We recall that the duration of the pulse is 1 ps. Taking this into consideration we conclude that the buildup and decay of the polarization, as illustrated in Figs. 4(a) and 4(b), occur in a field-free manner; e.g., the polarization is generated within 10 ps after the application of the pulse. It is also noteworthy that the magnitude of μ^{σ} is substantial [μ^{σ} in Figs. 4(a) and 4(b) is depicted in units of 10^6 D]. The maximum absolute value of the induced electric dipole moment decreases when shortening the relaxation time [see Fig. 4(a)]. Nevertheless, the post-pulse polarization is still appreciable within a typical range of values of τ_{rel} in ballistic semiconductor MR's (Ref. 1) as shown in Fig. 4(a). On the other hand, the induced dipole moment increases with the pulse field strength, but the time within which the polarization is formed decreases with stronger fields [see Fig. 4(b)]. Thus, the amount and duration of the induced dipole moment can, to a certain extent, be tuned by applying an appropriately designed HCP. In view of the above results it might appear tempting to increase the HCP field strength in order to enhance the amplitude of the induced polarization. It should be noted, however, that the treatment presented in this work is justified for relatively weak pulses which ensures that the energy delivered to the system is much smaller than E_F and the relaxation time approximation becomes viable.

The time evolution of the post-pulse dipole moment corresponding to an even number of spin-$\frac{1}{2}$ carriers has a damped oscillating behavior with nodes [see Eqs. (23), (25), and (31)] at $t=n\tau_p/N$ (with n being an integer number) and at those values of t for which $h(\Omega)=0$. Therefore the duration of the first half-cycle of the polarization (note that this cycle gives the strongest polarization, since the dipole moment is exponentially damped by the relaxation of the system) depends, essentially, on the number of carriers in the ring. This situation is illustrated in Fig. 5, where the time evolution of the induced dipole moment is displayed for different values of the number of particles in the ring.

The charge polarization depicted in Figs. 4 and 5 emerges after the HCP is diminished (the pulse duration is 1 ps). Thus the polarization buildup and decay occur in a nearly field-free environment. This observation can be exploited as a unique opportunity for investigating relaxation processes in the absence of external perturbations. The situation is qualitatively different from the case where a *stationary* polarization is induced by a dc electric field, because the switch-on and switch-off time of the dc field is usually very slow compared to τ_{rel}.

So far we have discussed results corresponding to the case in which a single HCP is applied. When the MR is subjected to a quasiperiodic train of HCP's (with period $T_p \gg \tau_{rel}$) the behavior of the time dependence of the polarization shown in Fig. 4 can be periodically repeated as many times as the number of applied pulses. This situation is displayed in Figs. 6(a) and 6(b) which show the time dependence of the induced polarization μ^{σ} corresponding to the case of a train of $k=10$ HCP's with period $T_p=100$ ps. In Figs. 6(a) and 6(b) the peak fields are, respectively, $F=1$ V/cm and $F=1$ kV/cm. It is worth mentioning that although we have limited our study to the case of a quasiperiodic train of unidirectional HCP's, it is also experimentally feasible to generate trains of bidirectional HCP's (Ref. 28) as well as the control of the time delay between consecutive pulses. Therefore it is possible to engineer the ring polarization on a picosecond time scale by appropriately designing the sequence of HCP's.

The radiation emission spectra corresponding to the polarization oscillations shown in Figs. 6(a) and 6(b) are dis-

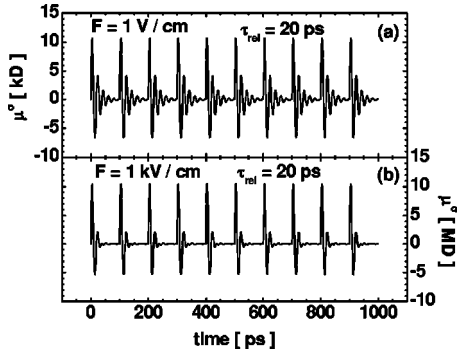

FIG. 6. Time dependence of the dipole moment μ^{σ} for the case of spin-$\frac{1}{2}$ particles. The results correspond to a train of $k=10$ HCP's with period $T_p=100$ ps.

played in Figs. 7(a) and 7(b), respectively. For the sake of comparison $I(\omega)$ has been expressed in the same arbitrary units in both Figs. 7(a) and 7(b). We note that the results depicted in Fig. 7(a) correspond to the case of very weak fields (i.e., for $F=1$ V/cm the condition $\alpha \ll 1/2$ holds). Therefore, the curves in that figure were computed by using the analytical expressions stated by Eqs. (37) and (39). Since for $F=1$ kV/cm, the condition $\alpha \ll 1/2$ is no longer valid, the results shown in Fig. 7(b) are obtained numerically by computing the Fourier transform according to Eq. (36). As anticipated in the previous section, the emission spectrum is composed of peaks at the integer harmonics ($\omega=n\omega_0$, $n=0,1,2,\ldots$) with amplitudes that are modulated by the modulation function $k^2Y(\omega)$. Thus, the system studied here can be useful for harmonic generation. The quantity $I(\omega)$ depends quadratically on the strength of the impulsive kicks mediated by the pulses to the system [see Eqs. (32)–(34)]. Therefore, the intensity of the emission lines increases with the peak field F. This behavior is particularly evident from a comparison of Figs. 7(a) and 7(b). The modulation function depends essentially on the ring parameters. Thus, by choosing appropriate values for ρ_0 and N one can *filter* (to a certain extent) some specific harmonics from the emission spectrum. For example, one can choose the system parameters such that ω_{max}/ω_0 coincides with the order of the harmonic one wishes to highlight [see Eq. (41) for the case of very weak

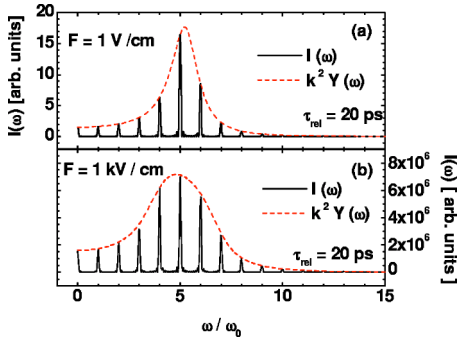

FIG. 7. (Color online) Emission spectrum (solid lines) and modulation function (dashed lines) for the case of spin-$\frac{1}{2}$ particles. The results correspond to a train of $k=10$ HCP's with period $T_p=100$ ps ($\omega_0=2\pi/T_p\approx 6.28\times 10^{10}$ Hz).

fields]. We also note that the charge polarization effects occur mainly between consecutive pulses and, therefore, in a field-free environment. This behavior is in contrast to the case in which a CW laser or symmetric laser pulses are used. In the case of CW lasers, the system is driven all the time by the external field and, therefore, no field-free charge oscillations occur. On the other hand, the post-pulse polarization strongly depends on the amount of momentum transferred by the external field to the system. This is the reason why HCP's should be employed instead of nearly symmetric laser pulses in order to be able to observe the effects discussed in the present work (a time-symmetric pulse transfers no net momentum to the system).

The emission spectrum displayed in Fig. 7 corresponds to charge oscillations that take place after the HCP's have faded away. Therefore, the emission spectrum contains information inherent to the properties of the system under zero external fields. This fact can be used as a tool for studying relaxation processes in absence of external perturbations. In fact, the results depicted in Fig. 7 hint on a method for measuring experimentally the relaxation time τ_{rel}. By measuring the emission spectrum, the relaxation time can be found as the value of τ_{rel} in the modulation function $k^2Y(\omega)$ that leads to the best correspondence with the emission peaks as determined experimentally. Furthermore, we believe that it is, in principle, possible to infer from the emission spectrum the existence or not of the various relaxation processes and their relevance. A definitive answer to this question, however, requires the detailed inclusion of the relaxation mechanisms. The proposed model includes the relaxation at a phenomenological level and cannot provide such a detailed information.

V. CONCLUDING REMARKS AND OUTLOOK

Summarizing we showed that when a thin ballistic MR is subjected to a single, linearly polarized HCP, a time-dependent charge polarization is induced in the ring. The induced polarization of the MR persists even after the HCP has passed by, i.e., under field-free conditions. The dependence of the field-free polarization induced in the ring on the pulse parameters was investigated. When a single HCP is applied, the MR charge polarization decays on a time of the order of the relaxation time of the system. Nevertheless, we have indicated that the charge polarization can be sustained for a longer time if an appropriate train of HCP's is utilized. The charge oscillations induced in that way can be engineered on the picosecond time scale by designing the pulse sequence in a predefined way. The emission spectrum generated by the induced charge oscillations was studied. The obtained results show the potentiality of the system investigated here as a tool for harmonic generation. A procedure was proposed for the experimental measurement of the time of relaxation of the excited states to the equilibrium state in absence of external perturbations.

The results are strictly valid for an *ideal* single-channel 1D ballistic ring. In these rings it has been shown that the electron-electron scattering is of a marginal importance for the stationary state due to the momentum conservation. Hence our treatment of the stationary system is well justified.

For the excited state the situation changes because, in general, the external field induces a charge polarization which breaks the rotational symmetry. Hence, the momentum conservation in the electron-electron scattering is violated. Thus, the excited ring resembles the situation encountered when going from clean to "dirty" metal rings in which the rotational symmetry is broken due to the presence of disorder. Therefore, the question arises as to the influence of the electron-electron interaction on our results which we treated on the basis of the relaxation time approximation. In general, the influence of the electronic interaction and disorder may affect qualitatively the properties of the rings. To contrast with our present case we recall the discussion following Eq. (10) where we showed explicitly that a weak pulse does not drive the system significantly far from the equilibrium and hence (in the studied case) the ground-state properties are not changed completely upon applying the pulse. To give some numbers for the studied case we note the following: applying a pulse with a peak field amplitude of 1 kV/cm leads to a maximal change of only 1.6 meV in the energy of an electron at the Fermi level. This value is considerably smaller than the Fermi energy $E_F = 38.2$ meV. Hence, we expect that including the effect of electronic correlation in a more sophisticated manner than within the relaxation time approximation will not alter qualitatively the essential findings of this study. We also recall that in the high-quality GaAlAs/GaAs MR used in the experiment of Ref. 15 the disorder was found to be very weak. For such ballistic rings the disorder effects are irrelevant. Nevertheless, in the authors view, it is highly interesting to study the emergence of electronic correlation effects as well as the influence of disorder in metallic rings and with increasing the strength of the pulses. In such a case the present analytical model is no longer justified and we have then to resort to full numerical simulations.

A further remark concerns the dimensionality of the ring. It is instructive to analyze whether the results of the single-channel 1D model offers a qualitatively correct picture for the electron dynamics in thin ballistic MR's with $\lambda_F < d \ll \rho_0$ and involving a small number $L (L \approx d/\lambda_F > 1)$ of radial channels. This is, for example, the case of the ring realized in the experiments of Ref. 15. For these thin rings and weak fields the angular and radial motion are adiabatically decoupled and the decisive effect of including the different radial channels is a lowering of the Fermi energy compared to the Fermi energy of the single-channel case. We expect that the peak of the polarization (see, for example, Fig. 4) will increase when other channels are included, since the system will be more easily excited (a similar situation occurs for the case of persistent currents, where the peak current scales as the square root of the number of channels[4,15]). On the other hand, lowering E_F is accompanied by a reduction of the angular velocity of the particles near the Fermi level and, consequently, one could expect the time oscillations of the single-channel polarization (see Fig. 4) to occur in a slower time scale when the different radial channels are included.

APPENDIX

Here we present some mathematical identities that were used in obtaining Eqs. (11), (6), (8), and (14). In all the identities e represents the Euler number, $m, n \in \mathbb{Z}$, and $a, b \in \mathbb{R}$.

$$J_m(a) \approx \frac{1}{\sqrt{2\pi m}} \left(\frac{ea}{2m} \right)^m, \quad m, a > 0, \quad m \gg a. \tag{A1}$$

The cases corresponding to negative values of m and/or a are easily obtained from Eq. (A1) by taking into account that $J_{-m}(a) = J_m(-a) = (-1)^m J_m(a)$:

$$\int_0^{2\pi} e^{im\theta} e^{ia \cos \theta} d\theta = 2\pi i^m J_m(a) = 2\pi i^m J_{-m}(-a), \tag{A2}$$

$$\sum_{m=-\infty}^{\infty} [m J_{n-m}(a)]^2 = n^2 + \frac{a^2}{2}, \tag{A3}$$

$$\sum_{m=-\infty}^{\infty} J_m(a) J_{m+1}(a) \begin{Bmatrix} \cos mb \\ \sin mb \end{Bmatrix} = J_1(\omega) \begin{Bmatrix} \sqrt{\frac{1-\cos b}{2}} \\ \frac{\sin b}{\sqrt{2(1-\cos b)}} \end{Bmatrix}, \tag{A4}$$

where $\omega = a\sqrt{2 - 2\cos b}$.

All the identities above were obtained, after some mathematical manipulations, from identities reported in Ref. 38.

[1] Y. Imry, *Introduction to Mesoscopic Physics*, 2nd ed. (Oxford University Press, Oxford, 2002).

[2] M. Büttiker, Y. Imry, and R. Landauer, Phys. Lett. **96A**, 365 (1983).

[3] R. Landauer and M. Büttiker, Phys. Rev. Lett. **54**, 2049 (1985).

[4] H. F. Cheung, Y. Gefen, E. K. Riedel, and W. H. Shih, Phys. Rev. B **37**, 6050 (1988).

[5] J. F. Weisz, R. Kishore, and F. V. Kusmartsev, Phys. Rev. B **49**, 8126 (1994).

[6] W. C. Tan and J. C. Inkson, Phys. Rev. B **60**, 5626 (1999).

[7] D. Loss and P. Goldbart, Phys. Rev. B **43**, 13 762 (1991).

[8] S. A. Washburn and R. A. Webb, Adv. Phys. **35**, 375 (1986).

[9] A. Müller-Groeling and H. A. Weidenmüller, Phys. Rev. B **49**, 4752 (1994).

[10] G. Bouzerar, D. Poilblanc, and G. Montambaux, Phys. Rev. B **49**, 8258 (1994).

[11] T. Chakraborty and P. Pietiläinen, Phys. Rev. B **50**, 8460 (1994).

[12] S. Latil, S. Roche, and A. Rubio, Phys. Rev. B **67**, 165420 (2003).

[13] L. P. Lévy, G. Dolan, J. Dunsmuir, and H. Bouchiat, Phys. Rev. Lett. **64**, 2074 (1990).

[14] V. Chandrasekhar, R. A. Webb, M. J. Brady, M. B. Ketchen, W. J.

Gallagher, and A. Kleinsasser, Phys. Rev. Lett. **67**, 3578 (1991).
[15] D. Mailly, C. Chapelier, and A. Benoit, Phys. Rev. Lett. **70**, 2020 (1993).
[16] W. Rabaud, L. Saminadayar, D. Mailly, K. Hasselbach, A. Benoît, and B. Etienne, Phys. Rev. Lett. **86**, 3124 (2001).
[17] K. B. Efetov, Phys. Rev. Lett. **66**, 2794 (1991).
[18] V. E. Kravtsov and V. I. Yudson, Phys. Rev. Lett. **70**, 210 (1993).
[19] O. L. Chalaev and V. E. Kravtsov, Phys. Rev. Lett. **89**, 176601 (2002).
[20] P. Kopietz and A. Völker, Eur. Phys. J. B **3**, 397 (1998).
[21] M. Moskalets and M. Büttiker, Phys. Rev. B **66**, 245321 (2002).
[22] K. Yakubo and J. Ohe, Physica E (Amsterdam) **18**, 97 (2003).
[23] G. M. Genking and G. A. Vugalter, Phys. Lett. A **189**, 415 (1994).
[24] N. E. Tielking, T. J. Bensky, and R. R. Jones, Phys. Rev. A **51**, 3370 (1995).
[25] R. R. Jones, D. You, and P. H. Bucksbaum, Phys. Rev. Lett. **70**, 1236 (1993); R. R. Jones, *ibid.* **76**, 3927 (1996); N. E. Tielking and R. R. Jones, Phys. Rev. A **52**, 1371 (1995); J. G. Zeibel and R. R. Jones, *ibid.* **68**, 023410 (2003); D. You, R. R. Jones, and P. H. Bucksbaum, Opt. Lett. **18**, 290 (1993).
[26] C. O. Reinhold, J. Burgdörfer, M. T. Frey, and F. B. Dunning, Phys. Rev. Lett. **79**, 5226 (1997); M. T. Frey, F. B. Dunning, C. O. Reinhold, S. Yoshida, and J. Burgdörfer, Phys. Rev. A **59**, 1434 (1999).
[27] S. Yoshida, C. O. Reinhold, and J. Burgdörfer, Phys. Rev. Lett. **84**, 2602 (2000).
[28] B. E. Tannian, C. L. Stokely, F. B. Dunning, C. O. Reinhold, S. Yoshida, and J. Burgdörfer, Phys. Rev. A **62**, 043402 (2000).
[29] A. Matos-Abiague and J. Berakdar, Appl. Phys. Lett. **84**, 2346 (2004); Phys. Rev. B **69**, 155304 (2004).
[30] C. M. Dion, A. Keller, and O. Atabek, Eur. Phys. J. D **14**, 249 (2001).
[31] N. E. Henriksen, Chem. Phys. Lett. **312**, 196 (1999).
[32] T. Swahn, E. N. Bogachek, Y. M. Galperin, M. Jonson, and R. I. Shekhter, Phys. Rev. Lett. **73**, 162 (1994).
[33] A. Matos-Abiague and J. Berakdar, Chem. Phys. Lett. **382**, 475 (2003); Phys. Rev. A **68**, 063411 (2003).
[34] J. M. Ziman, *Principles of the Theory of Solids*, 2nd ed. (Cambridge University Press, Cambridge, England, 1998).
[35] W. Jones and N. H. March, *Theoretical Solid State Physics* (Dover, New York, 1985), Vol. 2.
[36] M. Bayer, M. Korkusinski, P. Hawrylak, T. Gutbrod, M. Michel, and A. Forchel, Phys. Rev. Lett. **90**, 186801 (2003).
[37] R. J. Warburton, C. Schäflein, D. Haft, F. Bickel, A. Lorke, K. Karrai, J. M. García, W. Schoenfeld, and P. M. Petroff, Nature (London) **405**, 926 (2000).
[38] *Handbook of Mathematical Functions*, edited by M. Abramowitz and I. Stegun (Dover, New York, 1972).